PHYSICAL REVIEW B VOLUME 22, NUMBER 8 15 OCTOBER 1980

Optical properties of TiC_x ($0.64 \leq x \leq 0.90$) from 0.1 to 30 eV

D. W. Lynch, C. G. Olson, and D. J. Peterman
Ames Laboratory, U.S. Department of Energy and Department of Physics, Iowa State University, Ames, Iowa 50011

J. H. Weaver
Synchrotron Radiation Center, University of Wisconsin-Madison, Stoughton, Wisconsin 53589
(Received 30 October 1979)

The stoichiometry-dependent optical properties of bulk samples of TiC_x have been determined for four samples in the range $0.64 \leq x \leq 0.90$. Reflectance and absorptance data taken in the range 0.1–30 eV have been Kramers-Kronig analyzed to obtain the dielectric function and related functions. Interband absorption begins at 0.1 eV or less. The observed interband transitions are interpreted on the basis of existing energy-band calculations. Comparison of optical structure with joint-density-of-states calculations shows that the rigid-band model cannot be applied strictly to explain the x-dependent structure, especially in the 5–10 eV region. The electron-energy-loss functions exhibit two peaks, one near the free-electron plasmon energy and one near 10 eV, both peaks shifting to higher energy as x increases.

I. INTRODUCTION

Titanium carbide is one of a series of transition-metal carbides, nitrides, and oxides which have the rocksalt structure[1–3] typical of ionic insulators. They are metallic but are very hard and brittle, so there has been considerable controversy about the nature of the bonding. The electronic energy bands have been calculated a number of times, but, unfortunately, the resultant bands disagree and weight the importance of ionic, covalent and metallic bonding differently. The only tests of the calculated bands have been spectroscopic: soft x-ray absorption and emission spectra,[4] ultraviolet and x-ray photoemission spectra,[5–7] and optical spectra.[8,9] The optical spectra reported from the two previous investigations do not agree with each other, nor does either of them agree with what we have determined.

In this paper we report on the optical properties of bulk crystals of TiC_x measured over the energy range 0.1 to 30 eV, wider than that covered by previous investigations. These results are presented and compared with other spectra in Sec. III. The electron-energy-band calculations are summarized in Sec. II. A qualitative discussion of the optical spectra in terms of band calculations is given in Sec. IV.

II. BAND CALCULATIONS

Interest in the bonding of TiC and related compounds has stimulated many band calculations, beginning with the tight-binding bands of Bilz.[10] Ern and Switendick[11] calculated the bands by the augmented-plane-wave (APW) method, using a non-self-consistent potential derived from atomic charge distributions. Conklin and Silversmith[12] then made an approximately self-consistent APW calculation, obtaining results similar to those of Ern and Switendick. Lye and Logothetis[8] carried out a semiempiricial tight-binding calculation, while Alward *et al.*[9] made an empirical pseudopotential calculation, both groups having adjusted several parameters to give agreement between their calculated and measured reflectance spectra, spectra which disagree with those reported here. Neckel *et al.*[13–15] performed self-consistent APW calculations and used the results to interpret the soft x-ray emission spectra and the x-ray photoemission spectra (XPS) of TiC and seven other stucturally similar compounds.[16,17] Their energy bands for TiC are shown in Fig. 1. Trebin and Bross[18] used several different potentials in their modified APW calculations, getting general agreement with previous APW calculations. They also carried their calculations to higher energies, going over 1 Ry above the Fermi level. Ihara *et al.*[19] performed modified APW calculations also and showed the calculated bands over 1 Ry above E_F, but there are differences at higher energy between these and the Trebin-Bross bands. The latter have a gap or small overlap between the Ti $3d$-C $2p$ and the higher-lying Ti $4s$ states. Calais[20] has summarized all of the band calculations of TiC and similar compounds, including many cluster calculations not mentioned here.

In Fig. 1 we reproduce the bands of Neckel *et al.*[15] which we will use in our interpretation of the optical spectra. These bands are, in general, wider than those of either Conklin and Silversmith[12] or Ern and Switendick.[11] An examination of these three sets of bands shows that as self-consistency is approached the bands become wider. The X_1-X_1 energy difference is approximately 1.00, 1.10, and 1.15 Ry while the K_1-K_4 energy

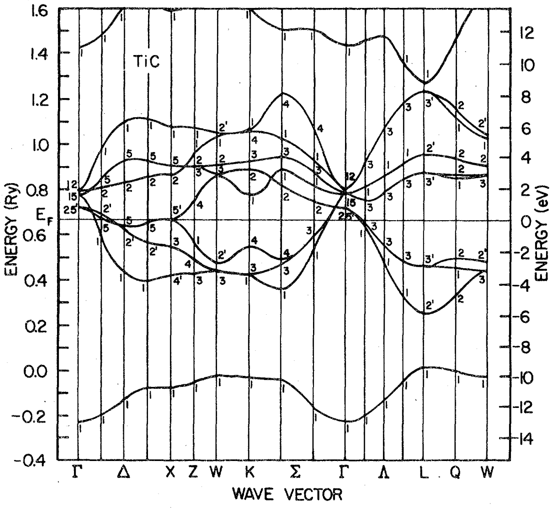

FIG. 1. Calculated electronic-energy bands of stoichiometric TiC (Ref. 15).

difference is 0.57, 0.58, and 0.64 Ry for the bands of Ern and Switendick, Conklin and Silversmith, and Neckel *et al.*, respectively. These differences will be shown to be important in Sec. IV when we consider the reciprocal-space origin of the optical structure.

III. EXPERIMENTAL RESULTS

Single crystals of TiC_x with $x = 0.833$, 0.90, and 0.97 were supplied by W. S. Williams of the University of Illinois-Urbana, and a polycrystalline, arc-melted sample with $x = 0.64$ was supplied by F. A. Schmidt of the Ames Laboratory. The latter crystal had traces (~5%) of a second phase since its average composition is close to the lower limit of the NaCl-structured phase. The single-crystal samples had natural (100) cleavage faces, while the polycrystalline sample was polished to a specular surface using diamond paste. All were electropolished before measurements, using 6% perchloric acid in methanol at ~200 K.

The measurements were made by two methods. From 0.1 to 4.2 eV a calorimetric technique, previously described,[21] was used to measure the absorptance A at 4.2 K. From 4 to 30 eV the reflectance, $R = 1 - A$, was measured at 300 K using synchroton radiation from the 240-MeV electron-storage ring Tantalus I at the Synchrotron Radiation Center of the University of Wisconsin. The method also has been descibed previously.[22] The accuracy of the measured absorptance or reflectance for the larger samples ($x = 0.64$ and 0.90) is better than 1% of A and 2–3% of R. The samples with $x = 0.833$ and 0.97 were too small for use in the low-temperature apparatus, while in the other, the measured reflectance spectra are multiplied by unknown, but constant, geometrical factors because of the small sample size.

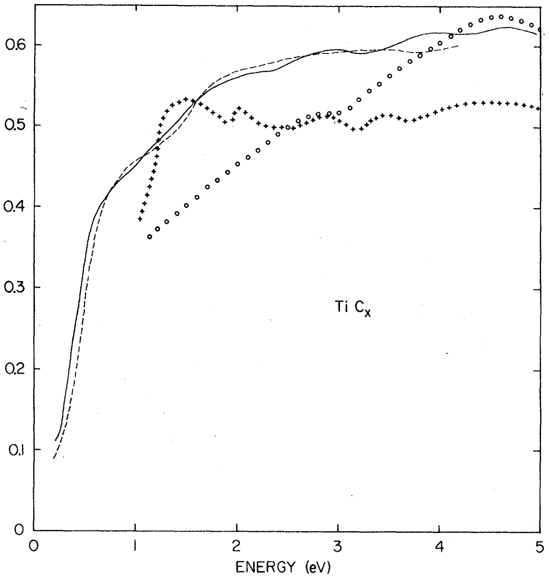

FIG. 2. Absorptance of TiC_x. Solid, this work, single crystal, $x = 0.90$, $T = 4.2$ K; dashed, this work, polycrystal, $x = 0.64$, $T = 4.2$ K; crosses, Ref. 9, sintered sample, $x = 0.999$, $T = 300$ K; circles, Ref. 8, single crystal, $x = 0.95$, $T = 300$ K.

Figure 2 shows the infared, visible, and near-ultraviolet absorptance at near-normal incidence for TiC_x ($x = 0.64$, 0.90). We also show the results of the two previous investigations of the optical properties of TiC. Those of Lye and Logothetis,[8] who used one of the same crystals ($x = 0.833$) used in our investigation, agree reasonably well with ours at higher energies but show poor agreement below 5 eV. The spectra of Alward *et al.*[9] were obtained on a sintered, mechanically polished sample which had been exposed to an argon discharge for *in situ* sputter etching. They report more structure than both Lye and Logothetis and we do, with maxima and minima at different energies. (Our bandpass was 0.03 eV at 1 eV, 0,06 eV at 2 eV, and 0.05 eV at 5 eV, sufficient to resolve such fine structure if it existed.) We note that our spectra on a number of samples form a series that varies in a smooth manner as the stoichiometry changes. Moreover, we have used the experimental methods outlined above on a large number of metallic samples, e.g., transition metals, and have obtained results in good agreement with data taken by other groups, using different methods.

The reflectances at higher energies are shown in Fig. 3. Our data agree fairly well with those of Lye and Logothetis, especially in the trends

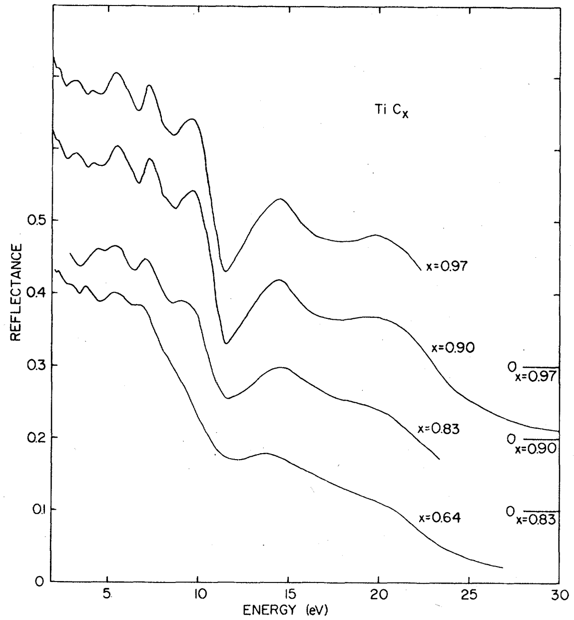

FIG. 3. Reflectance spectra of TiC$_x$ for several stoichiometries. See text for sample descriptions. Reflectance scales for $x = 0.83$ and 0.97 have been adjusted and are essentially arbitrary (see text).

seen as x decreases. In Fig. 3 the data for the $x = 0.833$ and 0.97 samples have been scaled, for the samples were too small for absolute measurements.

IV. DISCUSSION

Kramers-Kronig analyses were used to determine the complex dielectric function $\tilde{\epsilon} = \epsilon_1 - i\epsilon_2$ from the measured spectra with extrapolation to higher and lower energies. The absorptance below 0.1 eV was assumed to be that of a free-electron gas, the relaxation time of which was adjusted to match the measured absorptance at 0.1 eV. Note, however, that the low-energy data do not resemble the absorptance of a free-electron gas, making Kramers-Kronig analysis on an energy range smaller than ours difficult to carry out reliably. Between 30 and 90 eV data based on the absorption coefficient of Ti metal[23,24] were adjusted in magnitude to match the reflectance at 30 eV. Above 90 eV an extrapolation, $R(E)$ with R decreasing as the -3.5 power of the photon energy, was used; the dielectric function between 0.1 and 30 eV was relatively insensitive to the choice of the power. Since the 30–90 eV extrapolation may have underestimated the magnitude of R, as determined by our semiquantitative reflectance measurements in this spectral region, the ϵ_2 and conductivity spectra reported and the sum rule on ϵ_2 are best viewed as lower limits.

The results of the Kramers-Kronig analysis for the $x = 0.64$ and 0.90 samples are shown in Figs. 4–7. Figure 4 shows the real and imaginary parts of the dielectric function. Figure 5 shows the

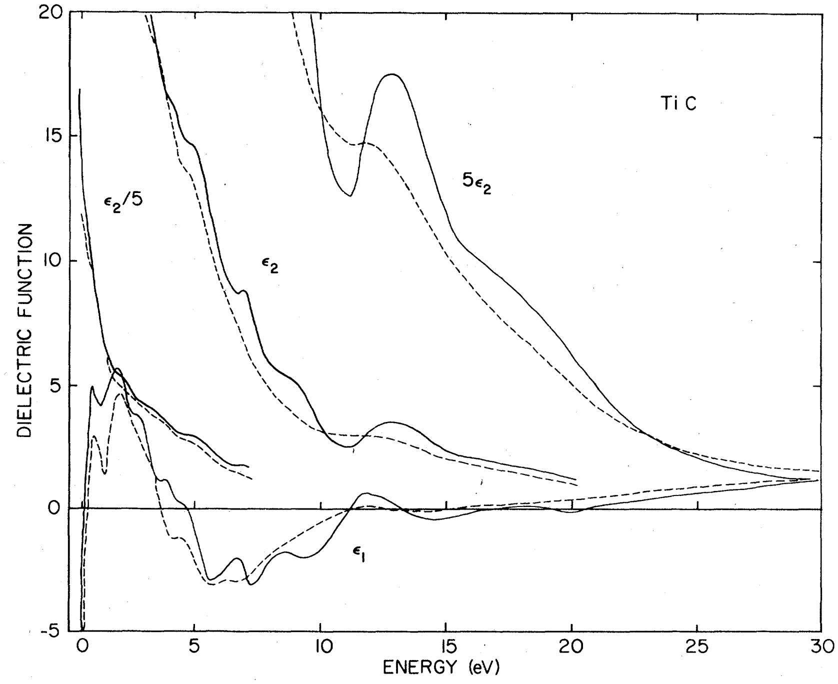

FIG. 4. Real (ϵ_1) and imaginary (ϵ_2) parts of the dielectric function for TiC$_x$ ($x = 0.64$, dashed, $x = 0.90$, solid) obtained from the data of Figs. 2 and 3 by the Kramers-Kronig analysis.

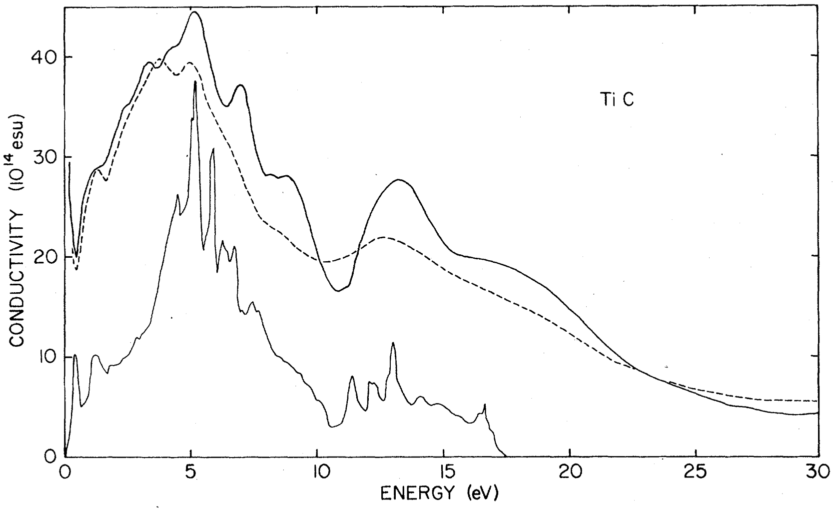

FIG. 5. Optical conductivity of TiC_x. Solid: $x=0.90$, dashed, $x=0.64$. Obtained from the data of Figs. 2 and 3 by Kramers-Kronig analysis. The lowest curve is the conductivity for $x=1$ calculated without dipole matrix elements from the bands of Ref. 15 (Fig. 1).

conductivity, $\sigma = \epsilon_2 E/4\pi\hbar$. Figure 6 shows the partial sum rule on ϵ_2,

$$N_{\rm eff}(E) = (2m\Omega/e^2h^2)\int_0^E E\epsilon_2(E)dE\ ,$$

with Ω the volume per "molecule" (TiC unit). $N_{\rm eff}$ is the number of electrons per molecule contributing to absorption (ϵ_2) below energy E. Figure 7 shows the volume and surface-electron-energy-loss functions, $\mathrm{Im}(-1/\tilde{\epsilon})$ and $\mathrm{Im}(-1/(\tilde{\epsilon}+1))$, respectively. These functions are proportional to the probability of excitation of a volume or surface longitudinal excitation at energy E, respectively. Some effects of interband absorption are already important at photon energies as low as 0.1 eV, so it has not been possible to separate out a free-electron contribution to the optical properties.

A comparison of the conductivity and the reflectance (Figs. 3 and 5) shows that there is a one-to-one correspondence of the interband structures, so that the trends seen in the reflectance spectra should carry over in the conductivity spectra, even for those samples whose absolute reflectances could not be measured, i.e., those for which Kramers-Kronig analyses were not carried out.

Changes in stoichiometry can give rise to a number of effects in the energy bands and the optical properties, not considering the concomitant lattice parameter change. For example, the rigid-band model predicts the Fermi level will drop as the carbon concentration decreases. Because the

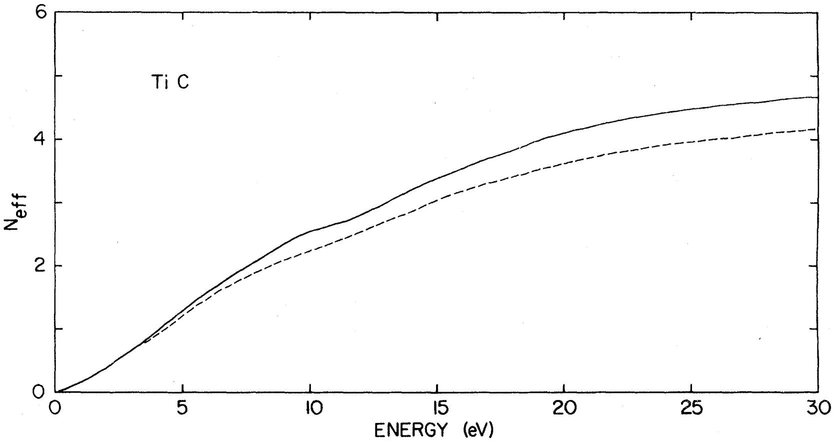

FIG. 6. Effective number of electrons per molecule contributing to absorption for below photon energy E is that energy determined from the partial sum rule. Solid, $x=0.90$; dashed, $x=0.64$.

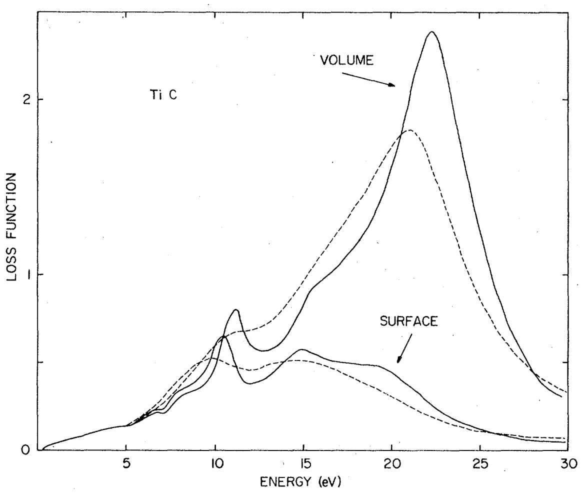

FIG. 7. Electron-energy-loss functions, $\mathrm{Im}(-1/\tilde{\epsilon})$ (volume) and $\mathrm{Im}[-1/(\tilde{\epsilon}+1)]$ (surface) for TiC_x. Solid, $x=0.90$; dashed, $x=0.64$.

density of states is so low, this drop could be appreciable, about 0.4 to 1.2 eV (depending on the band calculation) upon going from $x=0.94$ to $x=0.64$, using the density of states at the Fermi level for stoichiometric TiC, $x=1$, over the entire range. This shift would allow new transitions to occur, those with final states just above the Fermi level, and it would cause the loss of some transitions originating from states just below the Fermi level for $x=1$. Moreover, as the Fermi level drops, the states at E_F will change character due to hybridization changes, altering dipole matrix elements. The loss of translational symmetry as x decreases from unity could allow transitions which do not conserve wave vector, which would appear as a general broadening of the structures found when x is near unity, and possibly a change in strength in the interband region. The bands just below the Fermi level are composed largely of hybridized Ti 3*d* and C 2*p* states. The loss of carbon will leave "dangling bonds" in a localized picture, corresponding roughly to a flattening of the associated hybridized *p*-*d* bands, as well as broadening to account for scattering. The bands composed primarily of Ti 3*d* functions should change far less, although the loss of carbon could alter the crystal-field splitting. A recent paper treats non-stoichiometric TiC by the coherent potential approximation.[25]

There is a tendency toward broadening in the experimental spectra as the carbon concentration decreases, but it seems that scattering (nonconservation of wave vector) plays a secondary role. There is a loss of several structures upon decreasing x, particularly those at 7 and 9 eV (Fig. 3). Some of the lower-energy structures shift, broaden, and tend to merge with other structures so that unambiguous statements about their intensity changes are not possible. The broadening is evident also in the calculated densities of states and in the imaginary part of the self-energy.[25]

We have used an interpolation scheme with the energy eigenvalues of Ern and Switendick[11] and those of Neckel *et al.*[15] to obtain partial joint densities of states for pairs of bands. From this we hoped to locate the regions of k space for those structures in the 5–10 eV region for $x=0.97$, the stuctures which depend most upon the stoichiometry. In Fig. 5 we show the interband optical conductivity calculated from the bands of Neckel *et al.* without electric-dipole matrix elements. The structure calculated to be at 0.45 eV does not appear in the experimental conductivity spectrum, but the Drude contribution, which we have not subtracted from the experimental curve, may mask it. The sharp rise in the absorptance (Fig. 2) indicates that there is strong interband absorption at about 0.5 eV. It is clear that from 1 to 10.5 eV there is rather good agreement between the calculated conductivity and the experimental results, agreement extending even to the relative strengths of structures. All the transitions in this region are between the states in the bands derived from the Ti 3*d* and C 2*p* states, these transitions are exhausted at about 10.7 eV in both the measurements and the calculations. (When the narrower bands of Ern and Switendick[11] are used in a similar calculation of the conductivity the calculated minimum falls at 9.5 eV instead of 10.7 eV given by both experiment and the calculations of Ref. 15.) The transitions from 10 to 17 eV arise from the excitation of electrons from the C 2*s* band (the lowest band in Fig. 1) to states at and above the Fermi level. Here the calculated structures are too sharp and probably should be broadened before comparing with experiment, the broadening arising from a shorter lifetime for the deep holes in the C 2*s* band.

Many of the sharp peaks above 1 eV in Fig. 5 can be identified in the band structure of Fig. 1, but for many of the structures a unique assignment cannot be made without calculation of electric-dipole matrix elements. For example, the peak at 5.2 eV can arise from transitions of the type $W_2' \rightarrow W_3$, and $Q_1 \rightarrow Q_1$, Q_2, while those at 11.5 eV from $Q_1 \rightarrow Q_2$. A detailed list of assignments is probably misleading at this time.

Turning now to the dependence on stoichiometry we see that most of the changes occur above 5 eV. The transitions above 11 eV originate from the C 2*s* band. They are expected to weaken as x decreases, and this occurs. The shift to lower energy apparent in Fig. 5 may come from changes in the final states through changes in hydridization. Between 5 and 10 eV several structures weaken and broaden as x decreases. For these transitions we expect changes in hybridization, and those transitions depending on large amounts of C $2p$ character will weaken as x drops. The broadening is again apparent. The conductivity peak at 1.3 eV is puzzling, for it does not change. At such a low energy, it involves states near the Fermi level, and E_F changes upon lowering x. One explanation would be that it is a transition between flat bands which cross the Fermi surface. As the Fermi level drops, the energy between filled initial states and empty final states remains the same to the extent that the bands are really parallel. Figure 1 shows such transitions, $\Lambda_3 \rightarrow \Lambda_3$ at about 1 eV. The 3-eV peak, not really evident in the calculated conductivity, shifts about 0.5 eV over our range of stoichiometry. The bands of Fig. 1 predict the Fermi-level shifts by about 0.7 eV, implying the Fermi level is the initial state (the transition shifts to higher energy as the Fermi level drops). Recent photoemission data[26] indicate that the calculated hybridized C $2p$–Ti $3d$ bands are not wide enough. The fact that angle-integrated photoelectron spectra, which primarily reveal features in the filled density of states, exhibit no changes with stoichiometry[7,26] implicates the states above the Fermi level as changing with stoichiometry, rather than those below.

That dipole matrix elements are large, even though some of the excitations correspond to d-to-d transitions which are forbidden on the atom, can be seen from the sum rule on ε_2 shown in Fig. 6. About 4.5 electrons per molecule contribute to absorption below 30 eV. However, about 3 electrons per molecule contribute between 1 and 10 eV, the region of hybridized $d \rightarrow d$ transitions. There are 4 Ti ($4s^2 3d^2$) and 2 C ($2p^2$) electrons in the atoms, so well over half of the oscillator strength of these six electrons per molecule is exhausted by 10 eV, the limit of the pure valence-band transitions. The Ti $3d$ and C $2p$ states hybridize strongly, partly accounting for the large oscillator strength. (The Ti $4s$ states are empty in TiC but more $3d$ states are filled.) The C $2s$ electrons in band 1 begin to absorb at around 10 eV, but probably weakly, as judged by the change in slope of N_{eff}, and transitions from the Fermi level to the next set of bands begins around 11 eV. The onset of both these transitions gives rise to the minimum in reflectance at 11 eV and the small threshold in ϵ_2.

The band structure alone gives an excellent account of the overall optical properties without including dipole matrix elements. The x-dependent transitions at higher energy have been identified as excitations from the C $2s$ band. The effects of possible band narrowing are not evident in the measured spectra, but increased broadening is apparent as the stoichiometry deviates more from the ideal.

The electron-energy-loss spectra (Fig. 7) resemble those of a number of bcc and hcp transition metals in that there is a volume plasmon, the high-energy peak in $\text{Im}(-1/\tilde{\epsilon})$ at 22.6 eV and another peak at lower energy, 11.2 eV. The high-energy is very close to the calculated free-electron plasmon energy of 21.4 eV, calculated for $x = 0.90$ (including the $2s$ electrons of C). The high-energy peaks in the volume-loss function for $x = 0.90$ and 0.64 occur at an energy ratio of 22.6 eV/21.1 eV = 1.07. The ratio of free-electron-gas-plasma frequencies is 1.08 for these stoichiometries. The lower-energy peak for transition metals and TiC has not been interpreted with a microscopic model. It represents a screened longitudinal oscillation of the electrons which is not highly damped by interband transitions because it lies at a minimum in ϵ_2. There are also two peaks in the surface loss function, neither of which is related to the high-energy volume-loss peak by a factor of $\sqrt{2}$ because, below about 20 eV, TiC_x is not a free-electron-like system. The higher-energy peaks in $\text{Im}(-1/(\tilde{\epsilon}+1))$ are more damped in TiC than in transition metals. No electron-energy-loss data in TiC exist in the literature for comparison.

ACKNOWLEDGMENTS

This work was supported in part by the U. S. Department of Energy under Contract No. W-7405-Eng-82, Division of Materials Sciences, budget code AK-01-02-02-2 and in part by the National Science Foundation under Contract No. DMR 7821080. The single crystals of TiC_x were kindly supplied by Wendell S. Williams of the University of Illinois. The polycrystalline sample was produced by F. A. Schmidt of the Ames Laboratory. The storage ring is operated by the Synchrotron Radiation Center, University of Wisconsin-Madison, under Contract No. DMR 7721888 from the National Science Foundation. We thank K. H. Schwarz and A. C. Switendick for supplying us with a table of energy eigenvalues.

[1] E. K. Storms, *The Refractory Carbides* (Academic, New York, 1967).

[2] L. E. Toth, *Transition Metal Carbides and Nitrides* (Academic, New Yor, 1971).

[3] W. S. Williams, in *Progress in Solid State Chemistry*, edited by H. Reiss and J. O. McCaldin (Pergamon, New York, 1971), Vol. 6.

[4] D. W. Fisher and W. L. Baun, J. Appl. Phys. **39**, 4757 (1968).

[5] L. Ramquist, B. Esktig, E. Källne, E. Norland, and R. Manne, J. Phys. Chem. Solids, **30**, 1835 (1969); **30**, 1849 (1969); **31**, 2669 (1970).

[6] L. Ramquist, J. Appl. Phys. **42**, 2113 (1971).

[7] A. L. Hagström, L. I. Johansson, B. E. Jacobsson, and S. M. B. Hagström, Solid State Commun. **19**, 647 (1976); J. Elect. Spectros. **10**, 259 (1977); **11**, 75 (1977).

[8] R. G. Lye and E. M. Logothetis, Phys. Rev. **147**, 622 (1966).

[9] J. F. Alward, C. Y. Fong, M. El-Batanouny, and F. Wooten, Phys. Rev. B **12**, 1105 (1975); Solid State Commun. **17**, 1063 (1975).

[10] H. Bilz, Z. Phys. **153**, 338 (1958).

[11] V. Ern and A. C. Switendick, Phys. Rev. **137**, A1927 (1965).

[12] J. B. Conklin and D. J. Silversmith, Int. J. Quantum Chem. Suppl. **2**, 243 (1968).

[13] A. Neckel, K. Schwarz, R. Eibler, P. Weinberger, and P. Rastl, Ber. Bunsenges. Phys. Chem. **79**, 1053 (1975).

[14] P. Weinberger and A. Neckel, J. Phys. C **8**, 4001 (1975).

[15] A. Neckel, P. Rastle, R. Eibler, P. Weinberger, and K. Schwarz, J. Phys. C **9**, 579 (1976).

[16] P. Weinberger, Theor. Chim. Acta **42**, 169 (1976).

[17] P. Weinberger, Theor. Chim. Acta **44**, 315 (1977).

[18] H.-R. Trebin and H. Bross, J. Phys. C **8**, 1181 (1975).

[19] H. Ihara, Y. Kumashiro, and A. Itoh, Phys. Rev. B **12**, 5465 (1975).

[20] J.-L. Calais, Adv. Phys. **26**, 847 (1977).

[21] L. W. Bos and D. W. Lynch, Phys. Rev. B **2**, 4784 (1970).

[22] C. G. Olson and D. W. Lynch, Phys. Rev. B **9**, 3159 (1974).

[23] B. Sonntag, R. Haensel, and C. Kunz, Solid State Commun. **7**, 597 (1969).

[24] D. W. Lynch, C. G. Olson, and J. H. Weaver, Phys. Rev. B **11**, 3617 (1975).

[25] J. Klima, J. Phys. C **12**, 3691 (1979).

[26] J. H. Weaver and F. A. Schmidt, Phys. Lett. A **77**, 73 (1980).